

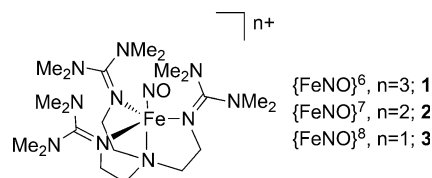
## Ferric NO Complexes

International Edition: DOI: 10.1002/anie.201601742  
German Edition: DOI: 10.1002/ange.201601742Structural and Spectroscopic Characterization of a High-Spin  $\{\text{FeNO}\}^6$  Complex with an Iron(IV)– $\text{NO}^-$  Electronic Structure

Amy L. Speelman, Bo Zhang, Carsten Krebs, and Nicolai Lehnert\*

**Abstract:** Although the interaction of low-spin ferric complexes with nitric oxide has been well studied, examples of stable high-spin ferric nitrosyls (such as those that could be expected to form at typical non-heme iron sites in biology) are extremely rare. Using the  $\text{TMG}_3\text{tren}$  co-ligand, we have prepared a high-spin ferric NO adduct ( $\{\text{FeNO}\}^6$  complex) via electrochemical or chemical oxidation of the corresponding high-spin ferrous NO  $\{\text{FeNO}\}^7$  complex. The  $\{\text{FeNO}\}^6$  compound is characterized by UV/Visible and IR spectroelectrochemistry, Mössbauer and NMR spectroscopy, X-ray crystallography, and DFT calculations. The data show that its electronic structure is best described as a high-spin iron(IV) center bound to a triplet  $\text{NO}^-$  ligand with a very covalent iron–NO bond. This finding demonstrates that this high-spin iron nitrosyl compound undergoes iron-centered redox chemistry, leading to fundamentally different properties than corresponding low-spin compounds, which undergo NO-centered redox transformations.

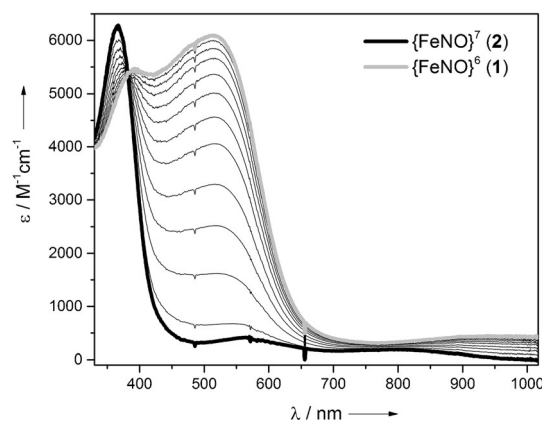
Nitric oxide ( $\text{NO}^\cdot$ ) is known to have a variety of effects in mammalian systems, where it acts as a signaling molecule at low (nanomolar) concentrations and as an immune defense agent at higher (micromolar) concentrations.<sup>[1]</sup> Many of the effects of nitric oxide are mediated by interaction with metal centers, particularly iron. Although the interaction of NO with both ferric and ferrous heme iron has been well-studied,<sup>[2]</sup> the interaction of NO with high-spin non-heme iron centers, particularly in the ferric case, is not as well understood. Correspondingly, although multiple low-spin (diamagnetic) ferric NO adducts ( $\{\text{FeNO}\}^6$  in the Enemark–Feltham notation)<sup>[3]</sup> are known in the literature, only one well-characterized high-spin (paramagnetic)  $\{\text{FeNO}\}^6$  complex has been reported to date.<sup>[4,5]</sup> However, this complex employs a tri-anionic tripodal thiolate ligand and is therefore dissimilar to typical biological non-heme iron sites. On the other hand, as has been shown previously, the neutral  $\text{TMG}_3\text{tren}$  ligand (1,1,1-tris[2-( $N^2$ -(1,1,3,3-tetramethylguanidino)ethyl]amine, Scheme 1) is able to stabilize iron in high oxidation states due to its strong donicity and typically favors

Scheme 1. Structure of the  $\text{TMG}_3\text{tren}$  iron nitrosyl complex.

high-spin electronic configurations.<sup>[7]</sup> This precedent suggests that it may be possible to generate a rare high-spin  $\{\text{FeNO}\}^6$  species (**1**) from the corresponding  $\{\text{FeNO}\}^7$  complex (**2**) previously reported by our group.<sup>[8]</sup>

Here, we report the synthesis of a high-spin  $\{\text{FeNO}\}^6$  complex  $[\text{Fe}(\text{TMG}_3\text{tren})(\text{NO})]^{3+}$  (**1**) generated via oxidation of **2**, which is the first example of a paramagnetic  $\{\text{FeNO}\}^6$  compound with a neutral co-ligand. This is also the first paramagnetic  $\{\text{FeNO}\}^6$  complex that can be characterized in the corresponding  $\{\text{FeNO}\}^7$  and  $\{\text{FeNO}\}^8$  oxidation states. The spectroscopic parameters and structural features of **1** are used to demonstrate that this complex is best described as a high-spin  $\text{Fe}^{\text{IV}}-\text{NO}^-$  species. Finally, the electronic structures of the set of  $\text{TMG}_3\text{tren}$   $\{\text{FeNO}\}^{6-8}$  complexes are contrasted to those of corresponding low-spin systems.

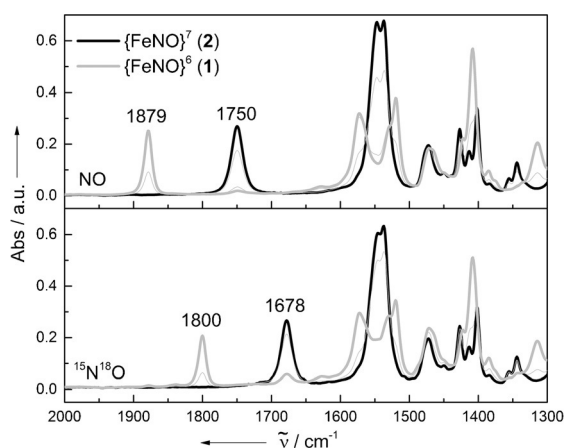
Previously, we reported that **2** undergoes a reversible one-electron reduction at  $-1.34$  V vs. ferrocene/ferrocenium to yield a metastable  $\{\text{FeNO}\}^8$  complex (**3**).<sup>[8]</sup> The cyclic voltammogram of **2** in acetonitrile also exhibits a chemically reversible  $\{\text{FeNO}\}^{6/7}$  couple at  $+0.67$  V vs. ferrocene/ferrocenium (Figure S1 in the Supporting Information). In order to determine the spectroscopic features of the oxidized compound (**1**), we first performed UV/Visible (Figure 1) and infrared (Figure 2) spectroelectrochemistry experiments.

Figure 1. UV/Visible spectroelectrochemistry showing the oxidation of **2** to **1** in  $\text{CH}_3\text{CN}$ .

[\*] A. L. Speelman, Prof. N. Lehnert  
Department of Chemistry, University of Michigan  
930 N University Avenue, Ann Arbor, MI 48109 (USA)  
E-mail: lehnertn@umich.edu

Dr. B. Zhang, Prof. C. Krebs  
Department of Chemistry, Department of Biochemistry and Molecular Biology, The Pennsylvania State University  
University Park, PA 16802 (USA)

Supporting information for this article can be found under:  
<http://dx.doi.org/10.1002/anie.201601742>.



**Figure 2.** IR spectroelectrochemistry showing the oxidation of **2** to **1** (top) and **2**- $^{15}\text{N}^{18}\text{O}$  to **1**- $^{15}\text{N}^{18}\text{O}$  (bottom) in  $\text{CD}_3\text{CN}$ .

In the UV/Vis spectrum, the high-intensity band at 365 nm ( $\epsilon = 6300 \text{ M}^{-1} \text{ cm}^{-1}$ ) in **2** is replaced by two features at 394 nm ( $\epsilon = 5400 \text{ M}^{-1} \text{ cm}^{-1}$ ) and 515 nm ( $\epsilon = 6100 \text{ M}^{-1} \text{ cm}^{-1}$ ) upon oxidation, corresponding to a color change from brown to deep red. A similar change in the absorption spectrum was reported for the oxidation of a  $\text{TMG}_3\text{tren Fe}^{\text{III}}\text{-CN}$  complex to an  $\text{Fe}^{\text{IV}}\text{-CN}$  complex; in this case, the high-intensity bands were assigned as LMCT bands originating from the  $\text{TMG}_3\text{tren}$  ligand.<sup>[7c]</sup> The analogous changes in UV/Vis features upon oxidation of **2** to **1** hint at an unusual  $\text{Fe}^{\text{IV}}$  oxidation state for **1** (since **2** is best described as an  $\text{Fe}^{\text{III}}\text{-NO}^-$  complex). Additionally, upon oxidation of **2** to **1** an extremely broad, low-intensity band grows in at ca. 980 nm ( $\epsilon \approx 440 \text{ M}^{-1} \text{ cm}^{-1}$ ). A similar feature has been observed in the  $\text{TMG}_3\text{tren Fe}^{\text{IV}}\text{=O}$  complex, and was assigned as an  $\alpha(d_{xz}/d_{yz} \rightarrow d_{z^2})$  transition,<sup>[7d]</sup> which further suggests that **1** could have a similar high-spin  $d^4$  electron configuration.

In the IR spectrum, the N–O stretch of **2** at  $1750 \text{ cm}^{-1}$  is replaced by a peak at  $1879 \text{ cm}^{-1}$  upon oxidation, which can be assigned as the N–O stretch based on comparison to the  $^{15}\text{N}^{18}\text{O}$  isotopolog. The magnitude of the upshift upon oxidation is nearly identical to the  $130 \text{ cm}^{-1}$  downshift observed in the iron-centered reduction of **2** to **3**,<sup>[8]</sup> implying that the oxidation of **2** to **1** is also iron-centered.

Complex **1** can be generated in bulk by chemical oxidation with the radical cation thianthrenyl tetrafluoroborate (see Figures S2–S4). The  $^1\text{H-NMR}$  spectrum of **1** exhibits broad,

paramagnetically shifted resonances (Figure S5) and a solution magnetic moment of  $3.2 \mu_{\text{B}}$  (determined using the Evans method) indicative of an  $S = 1$  spin state, which is consistent with the other reported paramagnetic  $\{\text{FeNO}\}^6$  complexes.<sup>[4,5]</sup>

In order to further characterize the series of  $\{\text{FeNO}\}^{6-8}$  complexes, Mössbauer spectra of frozen solutions of **1–3** were recorded (Table 1, Figures S6–S8). Due to the generally observed non-innocence of NO as a ligand, the redox state of the iron center cannot be definitively assigned by the isomer shift ( $\delta$ ) alone, since  $\delta$  is correlated with both Fe–ligand  $\pi$ -bonding and iron oxidation state.<sup>[9]</sup> However, the relatively large magnitude of the stepwise change in  $\delta$  along the  $\{\text{FeNO}\}^{6-8}$  series is suggestive of iron-centered redox chemistry (Table 1). Interestingly, both  $\delta$  and the quadrupole splitting ( $|\Delta E_{\text{Q}}|$ ) of **1** are extremely similar to the values for the  $S = 2$   $\text{TMG}_3\text{tren Fe}^{\text{IV}}\text{=O}$  complex.<sup>[7a]</sup> This similarity is due to the fact that  $\text{NO}^-$ , like the oxo ligand, acts as a strong  $\pi$ -donor in high-spin complexes (see below). This observation implies an  $\text{Fe}^{\text{IV}}\text{-NO}^-$  electronic structure for **1**. In contrast, the Mössbauer parameters of the  $S = 0$   $\text{TMG}_3\text{tren Fe}^{\text{IV}}\text{-CN}$  complex<sup>[7c]</sup> are significantly different from those of **1**.

Although it is unstable at room temperature, **1** is sufficiently stable at  $-35^\circ\text{C}$  to allow for crystallization (Figure 3, Table 1).<sup>[10]</sup> The Fe–N–O bond of **1** is completely linear, compared to the bent Fe–N–O bond of **2**<sup>[8]</sup> and other  $\{\text{FeNO}\}^7$  complexes.<sup>[11]</sup> Linearization of the Fe–N–O moiety in  $\{\text{FeNO}\}^6$  complexes has been observed previously for low-

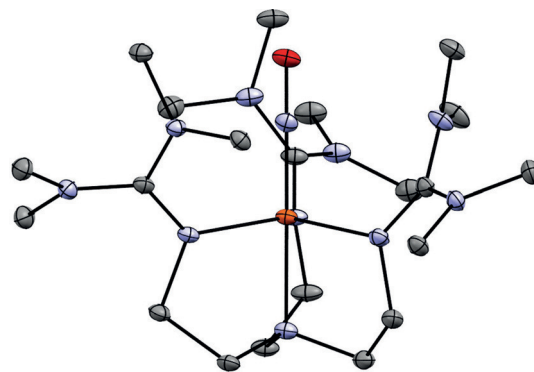


**Figure 3.** Crystal structure of **1** with thermal ellipsoids shown at 30% probability. Hydrogen atoms, solvent ( $\text{CH}_3\text{CN}$ ) molecules, and tetrafluoroborate counterions have been omitted for clarity. Color code: blue N, red O, orange Fe, gray C.

**Table 1:** Comparison of structural and spectroscopic parameters for the  $\text{TMG}_3\text{tren } \{\text{FeNO}\}^{6-8}$  series to selected compounds from the literature.

Compound	Fe–N [Å]	N–O [Å]	Fe–N–O [°]	Avg. Fe–N <sub>guan</sub> [Å]	Fe–N <sub>amine</sub> [Å]	S	$\delta$ [mm s <sup>-1</sup> ]	$ \Delta E_{\text{Q}} $ [mm s <sup>-1</sup> ]	$\nu(\text{NO})$ [cm <sup>-1</sup> ]	Ref. <sup>[e]</sup>
$\{\text{FeNO}\}^6$ , <b>1</b>	1.680	1.142	179.9	1.966	2.020	1	0.06 <sup>[a]</sup>	0.48 <sup>[a]</sup>	1879 <sup>[b]</sup>	<i>t.w.</i>
$\{\text{FeNO}\}^7$ , <b>2</b>	1.748	1.154	168.0	2.037	2.251	3/2	0.48 <sup>[a]</sup>	1.42 <sup>[a]</sup>	1750 <sup>[b]</sup>	[8], <i>t.w.</i>
$\{\text{FeNO}\}^8$ , <b>3</b>						1	0.84 <sup>[a]</sup>	2.78 <sup>[a]</sup>	1618 <sup>[b]</sup>	[8], <i>t.w.</i>
$[\text{Fe}^{\text{IV}}(\text{TMG}_3\text{tren})(\text{O})]^{2+}$				2.006	2.112	2	0.09 <sup>[c]</sup>	0.29 <sup>[c]</sup>		[7a,b]
$[\text{Fe}^{\text{IV}}(\text{TMG}_3\text{tren})(\text{CN})]^{3+}$						0	−0.19 <sup>[c]</sup>	4.45 <sup>[c]</sup>		[7c]
$\{\text{FeNO}\}^6$ [Fe(PS3*)(NO)]	1.676	1.154	175.2			1			1807 <sup>[d]</sup>	[4]
$\{\text{FeNO}\}^7$ [Fe(NS3)(NO)] <sup>−</sup>	1.756	1.11	145.9		2.178	3/2			1639 <sup>[d]</sup>	[4]
		1.18	147.8							

[a] Measured at 4.2 K in frozen 1:1 propionitrile:butyronitrile solution. [b] In  $\text{CH}_3\text{CN}$  solution. [c] Measured at 4.2 K in frozen  $\text{CH}_3\text{CN}$  solution. [d] Nujol mull. [e] *t.w.* = this work.

spin systems.<sup>[2]</sup> Oxidation leads to a decrease in the Fe–N(O) bond length in **1** as compared to **2**, whereas the N–O bond length is only marginally decreased in **1**. Although no structural characterization is available for the {FeNO}<sup>7</sup> form of [Fe(PS3\*)(NO)] (which is the only other structurally characterized paramagnetic {FeNO}<sup>6</sup> complex), the {FeNO}<sup>7</sup> form of the closely related complex [Fe(NS3)(NO)]<sup>–</sup> was structurally characterized; the geometric differences between the {FeNO}<sup>6</sup> and {FeNO}<sup>7</sup> compounds are qualitatively similar to those in **1** and **2** (Table 1).<sup>[4]</sup> Interestingly, the bonds to the TMG<sub>3</sub>tren coligand in **1** are much shorter than those reported for any other iron-TMG<sub>3</sub>tren structure, including the analogous Fe<sup>IV</sup>=O complex (Table 1) which again strongly implies an Fe<sup>IV</sup> center for **1**.<sup>[7b]</sup> Taken together, the structural and spectroscopic data all support the assignment of **1** as an Fe<sup>IV</sup>–NO<sup>–</sup> species.

To gain further insight into the nature of the bonding in this system, density functional theory (DFT) calculations were employed. The calculated geometric and spectroscopic parameters of **1**, **2**, and **3** are all in excellent agreement with experimental values (Tables S2–S3). In particular, the DFT-calculated and experimental  $\delta$  values show a strong linear correlation (Figure 4), which indicates that DFT is able to properly describe bonding trends within this series. As reported previously, the electronic structure of **2**<sup>[8]</sup> and other high-spin {FeNO}<sup>7</sup> complexes<sup>[11,12]</sup> is best described as a high-spin Fe<sup>III</sup> center antiferromagnetically coupled to triplet NO<sup>–</sup>. The NO<sup>–</sup> in these systems acts as a weak  $\pi$ -acceptor ( $\alpha$ -spin), but mainly as a strong  $\pi$ -donor ( $\beta$ -spin) into the iron d<sub>xz</sub> and d<sub>yz</sub> orbitals (where the z-axis lies along the Fe–N(O) bond vector), resulting in a highly covalent Fe–NO bond.<sup>[13]</sup> The DFT calculations reveal an Fe<sup>IV</sup>–NO<sup>–</sup> electronic structure for **1** consistent with experimental findings. Due to the higher effective nuclear charge of the iron center in **1** as compared to **2**, the NO<sup>–</sup> moiety donates additional electron density into the Fe d-orbitals in **1**, making the Fe–NO bond even more

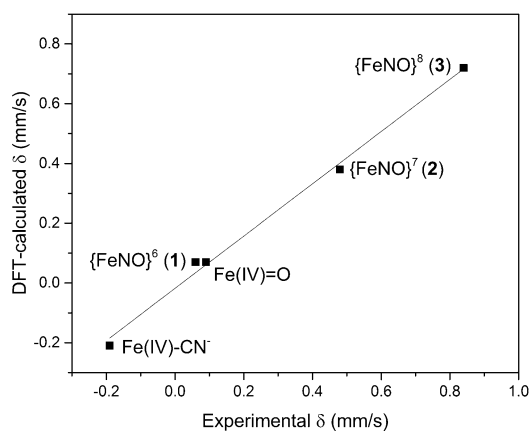


**Figure 4.** Correlation of experimental and DFT-calculated  $\delta$  (at the B3LYP level) for **1–3** and selected TMG<sub>3</sub>tren compounds (see Table 1).

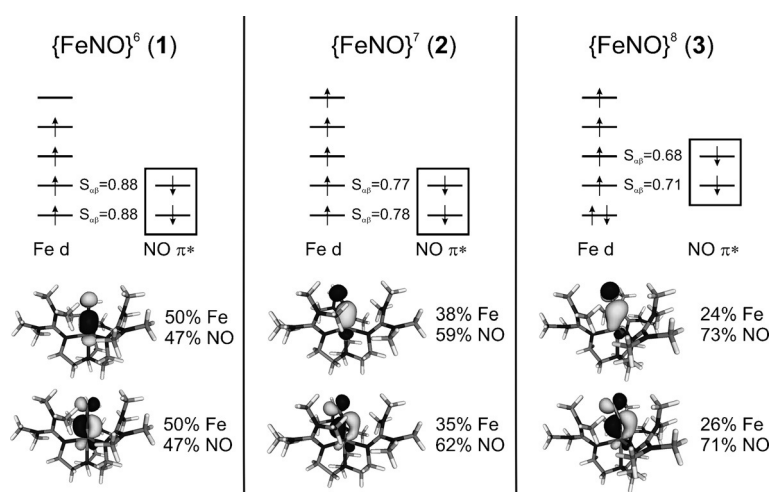


**Figure 5.** MO diagrams for the high-spin TMG<sub>3</sub>tren {FeNO}<sup>6–8</sup> series. The  $\beta$ -spin magnetic orbitals (boxed), which constitute the primary Fe–NO bonding interaction (NO<sup>–</sup> to Fe  $\pi$  donation), are shown with the percentage of iron and NO character indicated.  $S_{\alpha\beta}$  denotes the overlap between the  $\alpha$ -spin and  $\beta$ -spin orbitals and is an indicator of covalency in the Fe–NO unit (a larger  $S_{\alpha\beta}$  indicates a more covalent bond).

covalent. This finding is consistent with a previous study which showed that Fe–NO bond covalency increases with increasing effective nuclear charge of the iron center in a series of {FeNO}<sup>7</sup> complexes.<sup>[13]</sup> The increase in the covalency of the Fe–NO bond is reflected by the composition of the magnetic orbitals (Figure 5, bottom), where the orbitals of **1** show increased Fe character as compared to **2**. On the other hand, upon reduction of **2** to the {FeNO}<sup>8</sup> (Fe<sup>II</sup>–NO<sup>–</sup>) complex **3**, a decrease in the covalency of the Fe–NO bond is observed.

In contrast to the iron-centered redox chemistry for the high-spin complexes **1–3**, the redox chemistry in low-spin iron nitrosyl systems has been shown to be primarily NO-centered, which is supported by the spectroscopic features of these complexes. For example, in the [Fe(cyclam-ac)(NO)]<sup>n</sup> ( $n = 0, +1, +2$ ) system, N–O stretching frequencies of 1903 cm<sup>–1</sup>, 1607 cm<sup>–1</sup>, and 1271 cm<sup>–1</sup> and  $\delta$  values of 0.01 mm s<sup>–1</sup>, 0.26 mm s<sup>–1</sup>, and 0.41 mm s<sup>–1</sup> are observed for the {FeNO}<sup>6</sup>, {FeNO}<sup>7</sup>, and {FeNO}<sup>8</sup> complexes, respectively. The large changes in N–O stretching frequencies and small changes in  $\delta$  values are in accordance with more NO-centered redox chemistry in low-spin systems.<sup>[14]</sup> Heme complexes generally behave in a similar way. Thus, in heme systems, the N–O stretching frequencies for 5-coordinate {FeNO}<sup>6</sup>, {FeNO}<sup>7</sup>, and {FeNO}<sup>8</sup> complexes are approximately 1850 cm<sup>–1</sup>, 1680 cm<sup>–1</sup>, and 1460 cm<sup>–1</sup>, respectively.<sup>[2,15]</sup>

In the TMG<sub>3</sub>tren system, however, the N–O stretch increases only moderately (approximately 130 cm<sup>–1</sup>) upon oxidation, and the Mössbauer isomer shift decreases more significantly (approximately 0.4 mm s<sup>–1</sup>) in line with the fact that the redox chemistry is iron-centered. These results show how the electronic structures of iron nitrosyls are dependent on the spin state. We are currently investigating the reactivity differences that result from this. In particular, low-spin heme {FeNO}<sup>6</sup> complexes are known to be electrophilic due to their Fe<sup>II</sup>–NO<sup>+</sup> electronic structure.<sup>[2]</sup> In contrast, since **1** has an

Fe<sup>IV</sup>-NO<sup>-</sup> electronic structure and a highly covalent Fe-NO bond, the complex is not expected to be appreciably electrophilic. Additionally, low-spin {FeNO}<sup>6</sup> model complexes are intrinsically unstable with respect to NO loss,<sup>[2]</sup> whereas NO loss from **1** is not observed even under vacuum (Figure S9).

In summary, complexes **1–3** represent the first reported high-spin {FeNO}<sup>6–8</sup> series. Our data show that the {FeNO}<sup>6</sup>, {FeNO}<sup>7</sup>, and {FeNO}<sup>8</sup> complexes have Fe<sup>IV</sup>-NO<sup>-</sup>, Fe<sup>III</sup>-NO<sup>-</sup>, and Fe<sup>II</sup>-NO<sup>-</sup> electronic structures, respectively, indicating that in high-spin non-heme iron nitrosyl complexes of the form reported in this work, all readily accessible redox chemistry is iron-centered.

## Acknowledgements

This research was supported by the National Science Foundation (CHE-1305777 to N.L.) A.L.S. acknowledges support from an NSF Graduate Research Fellowship (DGE-0718128) and a Rackham Predoctoral Fellowship (University of Michigan). We acknowledge Dr. Jeff Kampf (University of Michigan) for the X-ray crystallographic analysis of **1** and the NSF for instrumentation (CHE-0840456).

**Keywords:** bioinorganic chemistry · enzyme models · nitric oxide · nitrogen oxides · non-heme iron

**How to cite:** *Angew. Chem. Int. Ed.* **2016**, *55*, 6685–6688  
*Angew. Chem.* **2016**, *128*, 6797–6800

- 
- [1] *Nitric Oxide: Biology and Pathobiology* (Ed.: L. J. Ignarro), Academic Press, San Diego, **2010**.
- [2] a) N. Lehnert, W. R. Scheidt, M. Wolf, *Struct. Bonding* **2013**, *154*, 155–223; b) M. D. Lim, I. M. Lorkovic, P. C. Ford, *J. Inorg. Biochem.* **2005**, *99*, 151–165.
- [3] In the Enemark–Feltham notation, metal nitrosyls are denoted by {MNO}<sup>X</sup> where X is the sum of metal d plus NO π\* electrons. See: J. H. Enemark, R. D. Feltham, *Coord. Chem. Rev.* **1974**, *13*, 339–406.

- [4] J. Conradie, D. A. Quarless, H.-F. Hsu, T. C. Harrop, S. J. Lippard, S. A. Koch, A. Ghosh, *J. Am. Chem. Soc.* **2007**, *129*, 10446–10456.
- [5] Two other {FeNO}<sup>6</sup> complexes have been suggested to be paramagnetic (*S* = 1), but in these cases the proposed spin state was not proven experimentally.<sup>[6]</sup>
- [6] a) M. J. Rose, N. M. Betterley, A. G. Oliver, P. K. Mascharak, *Inorg. Chem.* **2010**, *49*, 1854–1864; b) M. D. Pluth, S. J. Lippard, *Chem. Commun.* **2012**, *48*, 11981–11983.
- [7] a) J. England, M. Martinho, E. R. Farquhar, J. R. Frisch, E. L. Bominaar, E. Münck, L. Que, Jr., *Angew. Chem. Int. Ed.* **2009**, *48*, 3622–3626; *Angew. Chem.* **2009**, *121*, 3676–3680; b) J. England, Y. Guo, E. R. Farquhar, V. G. Young, Jr., E. Münck, L. Que, Jr., *J. Am. Chem. Soc.* **2010**, *132*, 8635–8644; c) J. England, E. R. Farquhar, Y. Guo, M. A. Cranswick, K. Ray, E. Münck, L. Que, Jr., *Inorg. Chem.* **2011**, *50*, 2885–2896; d) M. Srncic, S. D. Wong, J. England, L. Que, Jr., E. I. Solomon, *Proc. Natl. Acad. Sci. USA* **2012**, *109*, 14326–14331.
- [8] A. L. Speelman, N. Lehnert, *Angew. Chem. Int. Ed.* **2013**, *52*, 12283–12287; *Angew. Chem.* **2013**, *125*, 12509–12513.
- [9] M. Li, D. Bonnet, E. Bill, F. Neese, T. Weyhermüller, N. Blum, D. Sellmann, K. Wieghardt, *Inorg. Chem.* **2002**, *41*, 3444–3456.
- [10] Experimental details for the acquisition of crystal data and structure refinement can be found in the Supporting Information. CCDC 1450725 contains the supplementary crystallographic data for this paper. These data can be obtained free of charge from The Cambridge Crystallographic Data Centre via [www.ccdc.cam.ac.uk/data\\_request/cif](http://www.ccdc.cam.ac.uk/data_request/cif).
- [11] T. C. Berto, A. L. Speelman, S. Zheng, N. Lehnert, *Coord. Chem. Rev.* **2013**, *257*, 244–259.
- [12] C. A. Brown, M. A. Pavlosky, T. E. Westre, Y. Zhang, B. Hedman, K. O. Hodgson, E. I. Solomon, *J. Am. Chem. Soc.* **1995**, *117*, 715–732.
- [13] T. C. Berto, M. B. Hoffman, Y. Murata, K. B. Landenberger, E. E. Alp, J. Zhao, N. Lehnert, *J. Am. Chem. Soc.* **2011**, *133*, 16714–16717.
- [14] R. Garcia Serres, C. A. Grapperhaus, E. Bothe, E. Bill, T. Weyhermüller, F. Neese, K. Wieghardt, *J. Am. Chem. Soc.* **2004**, *126*, 5138–5153.
- [15] L. E. Goodrich, S. Roy, E. E. Alp, J. Zhao, M. Y. Hu, N. Lehnert, *Inorg. Chem.* **2013**, *52*, 7766–7780.

Received: February 18, 2016

Published online: April 21, 2016